Complex Frameshift Mutations Mediated by Plasmid pKM101: Mutational Mechanisms Deduced From 4-Aminobiphenyl-Induced Mutation Spectra in Salmonella

Jessie G. Levine,* Roel M. Schaaper† and David M. DeMarini‡,[1]

**Departmentof Environmental Sciences and Engineering, University of North Carolina at Chapel Hill, Chapel Hill, North Carolina 27599, †Laboratory of Molecular Genetics, National Institute of Environmental Health Sciences, Research Triangle Park, North Carolina 27709, and ‡Genetic Toxicology Division, U.S. Environmental Protection Agency, Research Triangle Park, North Carolina 27711*

Manuscript received July 19, 1993
Accepted for publication November 15, 1993

ABSTRACT

We used colony probe hybridization and polymerase chain reaction/DNA sequence analysis to determine the mutations in ~2,400 4-aminobiphenyl (4-AB) +S9-induced revertants of the −1 frameshift allele hisD3052 and of the base-substitution allele *hisG46* of *Salmonella typhimurium*. Most of the mutations occurred at sites containing guanine, which is the primary base at which 4-AB forms DNA adducts. A hotspot mutation involving the deletion of a CG or GC within the sequence CGCGCGCG accounted for 100 and 99.9%, respectively, of the reversion events at the *hisD3052* allele in the pKM101 plasmid-minus strains TA1978 (*uvr*$^+$) and TA1538 (Δ*uvrB*). In strain TA98 (Δ*uvrB*, pKM101), which contained the SOS DNA repair system provided by the pKM101 plasmid, ~85% of the revertants also contained the hotspot deletion; the remaining ~15% contained one of two types of mutations: (1) complex frameshifts that can be described as a −2 or +1 frameshift and an associated base substitution and (2) deletions of the CC or GG sequences that flank the hotspot site (CCGCGCGCGG). We propose a misincorporation/slippage model to account for these mutations in which (1) pKM101-mediated misincorporation and translesion synthesis occurs across a 4-AB-adducted guanine; (2) the instability of such a mispairing and/or the presence of the adduct leads to strand slippage in a run of repeated bases adjacent to the adducted guanine; and (3) continued DNA synthesis from the slipped intermediate produces a frameshift associated with a base substitution. This model readily accounts for the deletion of the CC or GG sequences flanking the hotspot site, indicating that these mutations are, in fact, complex mutations in disguise (*i.e.*, cryptic complex frameshifts). The inferred base-substitution specificity associated with the complex frameshifts at the *hisD3052* allele (primarily G·C → T·A transversions) is consistent with the finding that 4-AB induced primarily G·C → T·A transversions at the *hisG46* base-substitution allele. The model also provides a framework for understanding the different relative mutagenic potencies of 4-AB at the two alleles in the various DNA repair backgrounds of Salmonella.

THE determination of mutation spectra in reverse-mutation systems has provided considerable insights into mutational mechanisms, particularly those associated with frameshift mutation (RIPLEY 1990). The *hisD3052* allele of *Salmonella typhimurium*, which is a −1 frameshift that was induced by the acridine nitrogen mustard ICR-354-OH (OESCHGER and HARTMAN 1970; HARTMAN *et al.* 1986), has been used more than any other frameshift allele for the identification of mutagenic agents (KIER *et al.* 1986). In addition, the availability of this allele in strains containing different DNA repair backgrounds (INMAN *et al.* 1983; MARON and AMES 1983) has permitted the study of the influence of DNA repair on the mutability of this allele.

Various methods have been applied during the past 20 years to evaluate revertants of the *hisD3052* allele at the molecular level, including (1) deduction of the DNA sequence from the amino acid sequence of the histidinol dehydrogenase polypeptide coded by revertants of the *hisD3052* allele (ISONO and YOURNO 1974) and (2) cloning and DNA sequence analysis (FUSCOE *et al.* 1988; O'HARA and MARNETT 1991). However, the ability to analyze *hisD3052* revertants in numbers sufficient to construct informative mutation spectra has become practical only recently with the development of a colony probe hybridization procedure to identify a common hotspot mutation (KUPCHELLA and CEBULA 1991) and the application of polymerase chain reaction (PCR)/DNA sequence analysis to identify the remaining frameshifts (CEBULA and KOCH 1990b; KUPCHELLA and CEBULA 1991; BELL *et al.* 1991; DEMARINI *et al.* 1992). Thus, we have used these methods to examine the influence of DNA repair on the mutation spectrum of the *hisD3052* allele after reversion by a common environmental mutagen/carcinogen, 4-aminobiphenyl (4-AB), whose mutagenic potency at this allele is highly influenced by the DNA repair status of the cell.

[1] Author to whom correspondence should be addressed

4-AB is a well documented bladder carcinogen in laboratory animals and humans, and it is genotoxic in a wide variety of organisms and endpoints (IARC 1987a,b). More recent studies show that it is mutagenic in various strains of Salmonella (IOANNIDES *et al.* 1989) as well as in Drosophila (TRIPATHY *et al.* 1990) and mammalian cells (OLLER *et al.* 1989; BOOKLAND *et al.* 1992a,b). 4-AB also induces micronuclei (CLIET *et al.* 1989; SHELBY *et al.* 1989) and unscheduled DNA synthesis (ASHBY and MOHAMMAD 1988; STEINMETZ *et al.* 1988).

The metabolism of 4-AB via *N*-oxidation results in reactive electrophilic species capable of forming adducts with hemoglobin and DNA (BELAND and KADLUBAR 1990; KADLUBAR *et al.* 1991). Metabolically activated 4-AB forms a profile of DNA adducts that is similar in various species/tissues; the adducts are predominantly (70%) C(8) adducts on guanine, with minor adducts at the C(8) position of adenine (15%) and at the N^2 exocyclic position of guanine (5%) (BELAND and KADLUBAR 1990). Treatment of Salmonella strain TA1538 (*hisD3052, rfa, ΔuvrB*) with *N*-hydroxy-4-AB gives a similar adduct profile, with C(8) guanine accounting for 71% of the adducts (KADLUBAR *et al.* 1982).

Despite the wealth of studies demonstrating the carcinogenicity, mutagenicity, and DNA-adduct-forming ability of 4-AB, only one study has determined at the DNA sequence level the types of mutations induced by a DNA-reactive form of 4-AB. LASKO *et al.* (1988) sequenced 20 mutants of the *lacZα* gene fragment of *Escherichia coli* bacteriophage M13mp10 DNA treated with *N*-acetoxy-*N*-trifluoroacetyl-4-aminobiphenyl. As expected, G·C base pairs were the major targets for base-substitution mutations. The addition of an SOS DNA repair system provided by the pGW16 plasmid, which is a derivative of pKM101, was necessary for mutagenesis in the DNA nucleotide excision repair-proficient strain of *E. coli* used in the study. Transversions were a major class of mutation observed, although some frameshifts were also recovered.

The present study extends these observations by examining the role of DNA repair on the mutagenic specificity of this agent. As demonstrated by IOANNIDES *et al.* (1989), 4-AB is mutagenic at both a frameshift (*hisD3052*) and a base-substitution (*hisG46*) allele of Salmonella. Both of these alleles are available in strains that vary in their DNA repair background according to the presence or absence of nucleotide-excision repair (*uvrB*) and the presence or absence of the SOS DNA repair system provided by the pKM101 plasmid. Thus, we have constructed 4-AB-induced mutation spectra in five strains of Salmonella, involving two alleles and four different DNA repair backgrounds, permitting us to examine the influence of these factors on the mutagenic specificity of 4-AB.

The primary observation from this study is the enhanced frequency of 4-AB-induced complex frameshift mutations in the *hisD3052* strain carrying plasmid pKM101 (strain TA98). Each of these mutations can be described as a frameshift mutation with a flanking or nearby base substitution. We present a mutational model that accounts for these complex frameshifts as well as provides a framework for understanding the different mutagenic potencies of 4-AB in various DNA repair backgrounds.

MATERIALS AND METHODS

Mutagenicity assay: *S. typhimurium* strains TA1978 (*hisD3052, rfa*), TA1538 (*hisD3052, rfa, ΔuvrB*), TA98 (*hisD3052, rfa, ΔuvrB*, pKM101), TA1975 (*hisG46, rfa*), TA1535 (*hisG46, rfa, ΔuvrB*), and TA100 (*hisG46, rfa, ΔuvrB*, pKM101) were kindly provided by B. N. AMES, Biochemistry Department, University of California, Berkeley. Strains UTH8413 (*hisD3052, rfa*, pKM101) and UTH8414 (*hisG46, rfa*, pKM101) were provided by T. H. CONNER and T. S. MATNEY, Graduate School of Biomedical Sciences, University of Texas, Houston. The standard plate-incorporation assay (MARON and AMES 1983) was performed using three plates/dose and 10^8 cells/plate. After 3 days of incubation, the revertant colonies (rev) were counted, and the results were expressed as rev/plate. 4-AB (Sigma, St. Louis, Missouri) was diluted in dimethyl sulfoxide (DMSO, Burdick & Jackson, Muskegon, Michigan) and evaluated in the presence of Sprague-Dawley aroclor 1254-induced male rat liver S9 (1.8 mg of S9 protein/plate) that was prepared as described (MARON and AMES 1983).

Colony purification, DNA isolation, PCR and DNA sequencing: Approximately 2,200 *hisD3052* and 200 *hisG46* 4-AB-induced, independent revertants were streaked onto minimal medium supplemented with biotin (MARON and AMES 1983) and incubated for 2 days at 37° in order to purify each revertant clone and to assure that no nonrevertant cells from the background lawn were present. The target sequence of the *hisG46* allele is a CCC codon, and particular base substitutions at the first or second position of this codon produce the revertants described here. The purified revertants of the *hisG46* allele (strains UTH8414 and TA100) were analyzed by the colony probe hybridization procedure described by CEBULA and KOCH (1990a) with slight modifications. The probes were the 15-nucleotide oligomers described by CEBULA and KOCH (1990a). The filters were hybridized with the probes for 2 h at 37°; then the filters were washed in 3 × SSC (0.15 M NaCl and 0.015 M sodium citrate, pH 7.0) as follows: CTC, CAC and CCC at 47° for 25 min; TCC at 47° for 50 min; ACC at 50° for 20 min; and GCC at 55° for 24 min. Those revertants that hybridize to the probe containing CCC contain the original *hisG46* sequence; such revertants contain a suppressor mutation in the anticodon region of either of two $tRNA^{Thr}$ genes and represent a TA → GC transversion (KUPCHELLA *et al.* 1994).

Purified revertants of the *hisD3052* allele (strains TA1978, TA1538 and TA98) were first screened for the presence of a hotspot GC or CG deletion by means of the colony hybridization procedure described by KUPCHELLA and CEBULA (1991). The hybridization procedure was similar to that for the *hisG46* allele except that an additional unlabeled probe was used to enhance the hybridization reaction due to the presence of repeated sequences within the hotspot region (KUPCHELLA and CEBULA 1991).

Those revertants that did not contain the hotspot deletion were subjected to PCR and DNA sequence analysis as described by BELL *et al.* (1991). Briefly, revertant colonies were boiled for 10 min in 200 μl of TE buffer, centrifuged for 10 min, and 5–10 μl of the supernatant were used as the Salmonella genomic DNA in an asymmetric PCR in which the primers were present

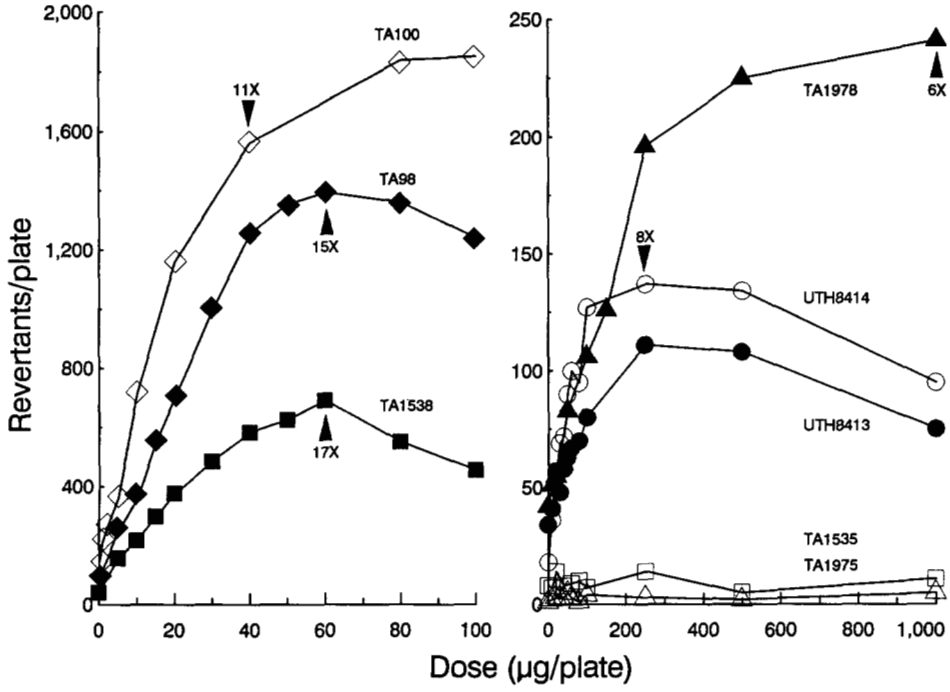

FIGURE 1.—Representative dose-response curves of 4-AB in the presence of S9 in eight strains of Salmonella. Open symbols, *hisG46* allele; filled symbols, *hisD3052* allele. Triangle, wild-type; square, *uvrB*; circle, pKM101; diamond, *uvrB* and pKM101. Arrows represent doses at which revertants were picked for molecular analysis. The fold increase over background is noted at each arrowhead.

TABLE 1

Mutagenic potency (revertants/μg) of 4-AB in Salmonella

	Frameshift (*hisD3052*)				Base substitution (*hisG46*)[a]	
Experiment	TA1978 (wild-type)	UTH8413 (pKM101)	TA1538 (Δ*uvrB*)	TA98 (Δ*uvrB*, pKM101)	UTH8414 (pKM101)	TA100 (Δ*uvrB*, pKM101)
1	0.4	0.5	12	19	1.4	51
2	1.0	0.7	13	29	1.1	37
3	0.6	0.6	12	24	1.7	42
Average	0.7	0.6	12	24	1.4	43

[a] 4-AB was not mutagenic at the *hisG46* allele in strains TA1975 (wild-type) and TA1535 (Δ*uvrB*), which did not contain pKM101 (Figure 1); thus, mutagenic potencies could not be calculated for 4-AB in these two strains.

at a ratio of 1:100. After 40 cycles of heating and cooling, the reaction was subjected to ultrafiltration, and the amplified ssDNA was sequenced using dITP termination mixes by the method of SANGER *et al.* (1977).

Statistical analysis: Statistical comparisons of the *hisD3052* mutation spectra were performed using the program of ADAMS and SKOPEK (1987), which produces a Monte Carlo estimate of the *P* value of the hypergeometric test (a generalization of Fisher's exact test). Comparisons of the *hisG46* mutation spectra were performed by chi-square analysis using the Stat-Sak program (GERARD E. DALLAL, 53 Betran Street, Malden, Massachusetts 02148).

RESULTS AND DISCUSSION

Dose-response curves and mutagenic potency: Figure 1 shows representative 4-AB-induced mutagenicity dose-response curves from which revertants were picked for analysis. Mutagenic potencies, calculated from the slope of the linear portions of these curves, are listed in Table 1 for the set of experiments reported in this study. For the frameshift allele *hisD3052*, the average mutagenic potency of 4-AB in the excision repair-proficient strain TA1978 was 0.7 rev/μg. Addition of the pKM101 plasmid did not cause much change in the mutagenic potency (0.6 rev/μg). However, the excision repair-deficiency in strain TA1538 (Δ*uvrB*) increased the potency of 4-AB by ~17-fold (12 *vs.* 0.7 rev/μg). The combination of nucleotide excision-repair deficiency (Δ*uvrB*) and the presumed error-prone translesion synthesis provided by the pKM101 plasmid (strain TA98) doubled this value to 24 rev/μg.

4-AB was unable to revert the base-substitution allele *hisG46* in the absence of the plasmid regardless of the nucleotide excision-repair background (strains TA1975 and TA1535 in Figure 1). In the presence of the plasmid (strain UTH8414), 4-AB induced 1.4 rev/μg; whereas, the combination of nucleotide excision-repair deficiency and plasmid pKM101 (strain TA100) increased the mutagenic potency to 43 rev/μg (Figure 1 and Table 1). Our results for strains TA1535, TA1538, TA98 and TA100 are similar to those reported in other studies (HAWORTH *et al.* 1983; STEELE and IOANNIDES 1986; IOANNIDES *et al.* 1989; IARC 1987a); results for 4-AB in strains TA1978, UTH8413 and UTH8414 have not been reported previously. These results show that 4-AB reverts both alleles, especially in the absence of the uvrABC

TABLE 2

Number (%) and class of mutational events at the *hisG46* allele

Condition	Total mutants	TCC	ACC	GCC	CTC	CAC	CCC
UTH8414							
Background	109	17 (15.6)	19 (17.4)	2 (1.8)	26 (23.9)	42 (38.5)	3 (2.8)
4-AB	99	4 (4.0)	26 (26.2)	0 (0.0)	9 (9.1)	59 (59.6)	1 (1.0)
TA100							
Background	192	22 (11.5)	30 (15.6)	7 (3.6)	39 (20.0)	90 (46.9)	4 (2.0)
4-AB	94	6 (6.4)	23 (24.5)	1 (1.0)	13 (13.8)	51 (54.0)	0 (0.0)

excision-repair system. Although 4-AB is mutagenic at the *hisD3052* allele in the presence or absence of plasmid pKM101, the plasmid is required for all 4-AB-induced mutagenesis at the *hisG46* allele.

The fold over background at which revertants were picked for molecular analysis is indicated by arrows in Figure 1. Revertants of wild-type strain TA1978 were picked at 1000 μg/plate, which was considerably higher than the doses at which revertants were picked for the other strains, but there was no indication of toxicity at this high dose. Other than for strain TA1978, for which ~84% of the revertants were induced by 4-AB (based on a 6-fold increase over the number of background revertants), greater than 93% of the revertants in the other strains were induced by 4-AB.

Mutation spectrum at the *hisG46* allele: The base-substitution mutational specificity of 4-AB at the *hisG46* allele was determined by analyzing background and 4-AB-induced revertants of UTH8414 (pKM101) and TA100 (Δ*uvrB*, pKM101) selected at 8- and 11-fold, respectively, over the background (Figure 1). The number of revertants analyzed and the number (and percentage) in each category are shown in Table 2. The yield of revertants in each category is shown in Figure 2. The results showed that 78% (TA100) to 86% (UTH8414) of the base substitutions induced by 4-AB at the *hisG46* allele were G·C → T·A transversions. Chi square analysis indicated that the background and 4-AB-induced mutation spectra (Figure 2) were significantly different in UTH8414 ($\chi^2 = 18.03$, $P = 0.002$) as well as in TA100 ($\chi^2 = 52.90$, $P < 0.001$). Not surprisingly, the 4-AB-induced mutation spectra were significantly different between the two strains ($\chi^2 = 16.16$, $P = 0.006$) because the excision-repair deficiency in TA100 increased the mutant yield by 10-fold. In contrast, the background mutation spectra were not significantly different between the two strains ($\chi^2 = 5.04$, $P = 0.41$).

The finding that the majority of the 4-AB-induced base substitutions in these pKM101-containing strains were G·C → T·A transversions is consistent with previous studies using other mutagens or background mutants in *E. coli* (Fowler *et al.* 1979; Mattern *et al.* 1985) and Salmonella (Eisenstadt *et al.* 1989; Cebula and Koch 1990a; Prival and Cebula 1992) that show that the

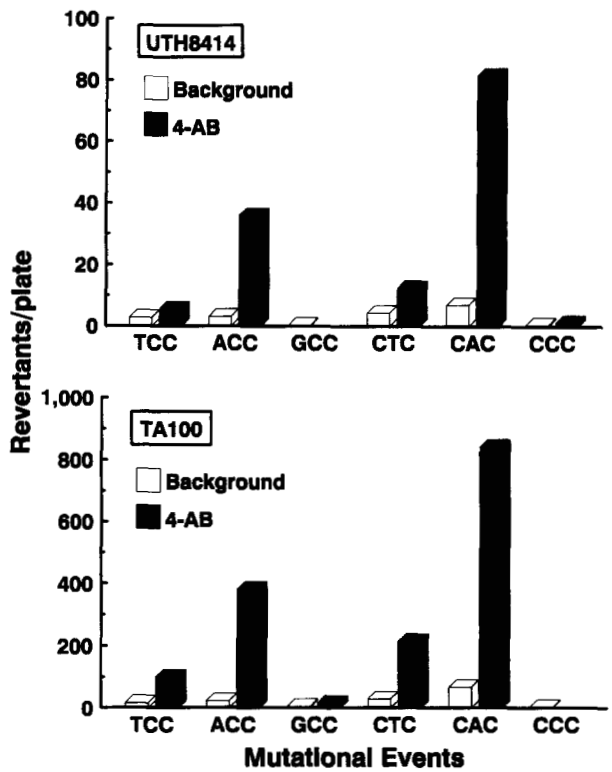

Figure 2.—Distribution of base-pair substitutions at the *hisG46* allele recovered among background (open bars) and 4-AB-induced (filled bars) revertants of strains UTH8414 (pKM101) and TA100 (Δ*uvrB*, pKM101) of Salmonella in the presence of S9. Revertants were picked at the doses and the fold increases over the background indicated by arrows on the dose-response curves in Figure 1. The CCC class represents reversion events at an extragenic suppressor tRNA, and CCC is the target sequence of the *hisG46* allele. The rev/plate of each class of mutation were calculated by distributing the total number of rev/plate obtained under each condition (Figure 1) among the classes of mutations based on the frequency (%) at which each class of mutation occurred (Table 2). The total rev/plate for UTH8414 were 18 (control) and 137 (4-AB); for TA100 they were 144 (control) and 1560 (4-AB).

pKM101 plasmid primarily enhanced the frequency of transversions. Likewise, Lasko *et al.* (1988) found that most of the *N*-hydroxy-4-AB-induced mutants in bacteriophage M13mp10 were also transversions and required the presence of the pKM101-derived plasmid pGW16.

Mutation spectra and classification of mutants at the *hisD3052* allele: The 4-AB-induced mutation spectra at

the *hisD3052* allele in three DNA repair backgrounds are shown in Figure 3. The frequencies at which various classes of mutations were recovered in each strain are shown in Table 3. A complete mutation spectrum was not constructed for revertants of strain UTH8414 (pKM101) because 4-AB induced a mutant yield in this strain that was only 3-fold above the background, preventing the construction of a meaningful mutation spectrum. However, we determined the frequency of the hotspot mutation in this strain, which was 25% for the background and 65% for 4-AB.

In the wild-type strain (TA1978), the hotspot mutation (–CG or –GC at CGCGCGCG) accounted for 87.4% of the total. Among the remaining mutations, nearly twice as many duplications as deletions were recovered; whereas, no insertions or complex mutations (frameshifts involving a base substitution, see below) were recovered. Among the deletions and duplications, a wide range of sizes was observed, including the largest deletion (35 bases) and the largest duplication (46 bases) detected in any strain in this study.

Only one of the 396 revertants in the TA1978 mutation spectrum was a true revertant, *i.e.*, one that reverted by the addition of a C at the site of the original –C mutation in this allele (the missing C is noted by a dash after nucleotide 893 in Figure 3). The frequencies and types of mutations induced by 4-AB were estimated by subtracting the background mutation spectrum using the method described in the legend of Table 4. The 4-AB-induced revertants of strain TA1978 were picked at 6-fold over the background. Thus, it was probable that one mutation out of six (*i.e.*, 66 of the 396 mutations) was actually a background mutation. After subtracting the background (Table 4), we determined that 4-AB induced only the hotspot deletion in TA1978; the other mutations present in the spectrum were presumptive background mutations.

The absence of nucleotide excision repair (strain TA1538) strongly increased the mutagenic potency of 4-AB and permitted analysis of revertants selected at 18-fold above background. This resulted in a 4-AB-induced spectrum that was composed nearly entirely of the hotspot deletion (99.3%). Of 912 revertants analyzed, only 6 non-hotspot mutations were recovered, 5 of which were deletions, and the remaining one was a complex mutation (discussed below). No large duplications were observed in this (or the TA98) spectrum due to the large increase above the background produced by 4-AB in the *uvrB* strains and the relatively low background frequency of duplications in the *uvrB* strains (Table 4). After subtracting the background mutations (Table 4), we determined that 4-AB induced primarily the hotspot deletion (along with the single complex mutation) in this strain.

The spectrum of 4-AB-induced revertants in strain TA98, which contained the error-prone translesion synthesis capability provided by the pKM101 plasmid, contained many more complex frameshift mutations, most of which can be defined as (+1) or (–2) frameshifts associated with a flanking base substitution, *e.g.*, CGC → A at position 880–882 (Figure 3). As argued below, this class also includes the apparent deletion of the CC or GG flanking the hotspot site, which we consider to be cryptic complex frameshifts. After subtracting the background revertants from this spectrum (Table 4), we determined that 4-AB induced only two classes of mutations: the hotspot deletion (~85%) and the complex frameshifts (~15%). The complex mutations occurred primarily at two sites and consisted of either (1) a 2-base deletion and a contiguous base substitution at the hotspot, (2) the apparent deletion of the CC or GG that flank the hotspot site, or (3) a 1-base duplication and a base substitution separated by one base at the TGA stop codon 3′ from the hotspot site (Figure 3).

Hotspot mutations at the *hisD3052* allele: Since the initial work of Isono and Yourno (1974), evidence has accumulated showing that a large percentage of the spontaneous and induced revertants of the *hisD3052* allele revert as a result of a hotspot mutation, which consists of a 2-base deletion (–CG or –GC) within the sequence CGCGCGCG (Fuscoe *et al.* 1988; Cebula and Koch 1990a; Bell *et al.* 1991; Kupchella and Cebula 1991; O'Hara and Marnett 1991; DeMarini *et al.* 1992). Based on the analysis above, the 4-AB-induced revertants of this allele are no exception (Table 4).

The high frequency of hotspot mutations induced by 4-AB is typical of other polycyclic planar mutagens with reactive side groups that permit the formation of DNA adducts. A previous study by Isono and Yourno (1974) that was confirmed by Kupchella and Cebula (1991) showed that 5 out of 5 4-nitroquinoline-*N*-oxide-, 6 out of 6 2-nitrosofluorene-, and 5 out of 5 hycanthone-induced revertants contained this hotspot mutation. Fuscoe *et al.* (1988) found this mutation among 5 out of 5 PHIP-, 13 out of 13 IQ-, 3 out of 3 MeIQ-, and 3 out of 3 aflatoxin B1-induced revertants.

With the development of colony probe hybridization procedures to simplify the identification of the hotspot mutation (Kupchella and Cebulla 1991), larger sample sizes (200 or more induced revertants) have been analyzed. Cebula and Koch (1990b) found that 97% of Adriamycin-, 92% of daunomycin-, 86% of aflatoxin B1-, 92% of *N*-2-acetylaminofluorene- (2-AAF), and 74% of benzo(*a*)pyrene-induced revertants contained the hotspot mutation. A recent review of work from our laboratory (DeMarini *et al.* 1993) shows that 86% of ellipticine-, 94% of 1-nitropyrene-, 98% of Glu-P-1-, 89% of main- and side-stream cigarette smoke condensate-, 90% of urban air particulate organic-, and 88–98% of municipal waste incinerator particulate organic-induced revertants contained the hotspot mutation.

Three exceptions to this general trend have been

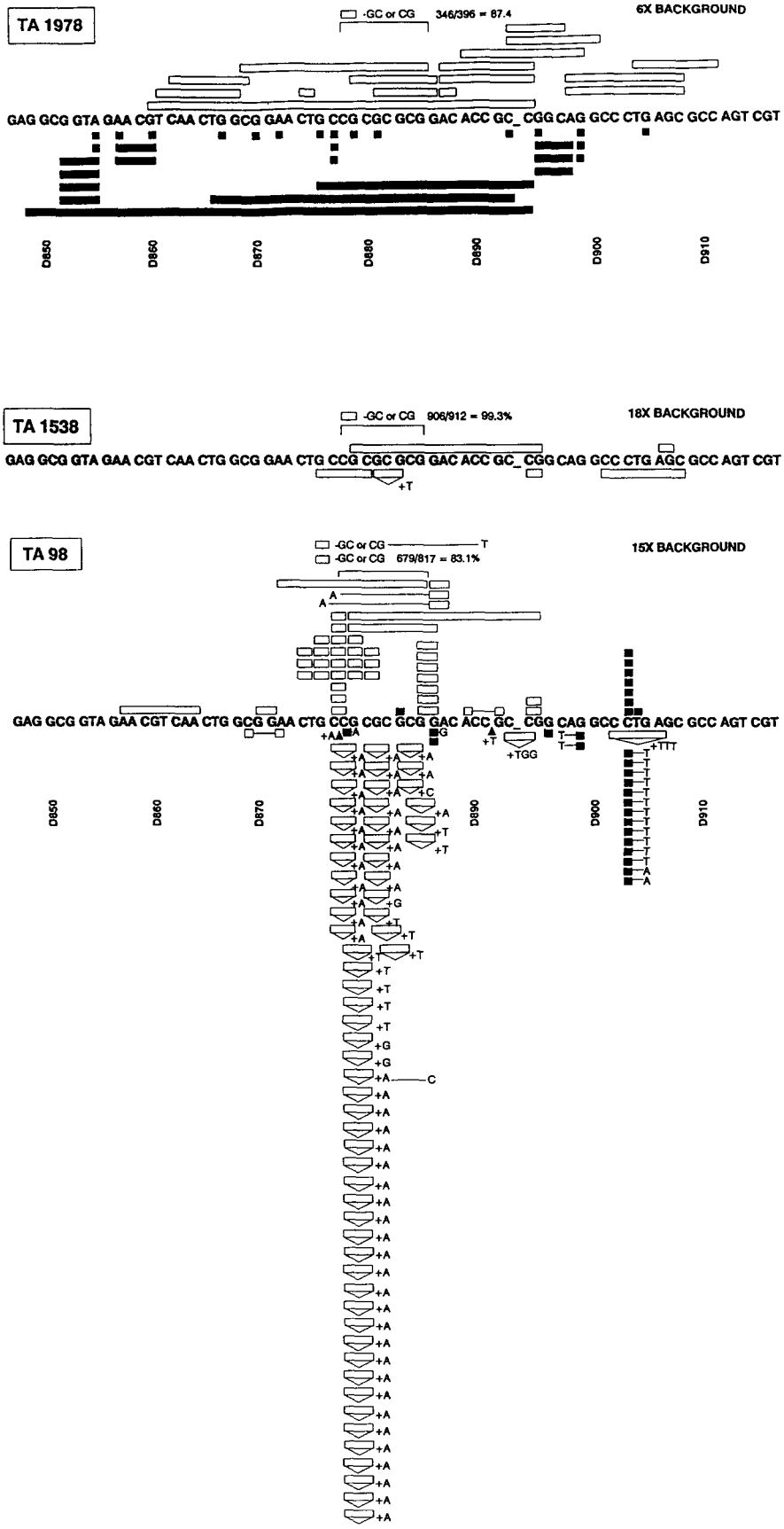

FIGURE 3.—Mutation spectra of 4-AB-induced revertants of strains TA1978, TA1538 and TA98 of Salmonella in the presence of S9. The dash after position 893 represents the −1 deletion of a C that constitutes the *hisD3052* allele. Open bars, deletions; filled bars, duplications; open bars with attached triangles, complex mutations involving deletion, addition, and/or base substitution; mutations connected by a line, complex mutations involving deletion or duplication plus a base substitution at a nearby site. Each symbol represents the mutation present in a single revertant. The TA1538 and TA98 spectra were each composed of three separate collections of revertants. Application of the statistical program of ADAMS and SKOPEK (1987) showed that the three spectra generated for a particular strain were not significantly different ($P > 0.5$); thus, they were combined to form the spectra shown here.

TABLE 3

Percentage (frequency) of classes of mutations in 4-AB mutation spectra at the *hisD3052* allele

Mutation class	TA1978 (wild-type)	TA1538 (Δ*uvrB*)	TA98 (Δ*uvrB*, pKM101)
Deletions			
Hotspot[a]	87.4 (346/396)	99.3 (906/912)	83.1 (679/817)
Other			
-2	0.5 (2/396)	0.2 (2/912)	0.5 (4/817)
-5	0.5 (2/396)	0.1 (1/912)	
-8	1.8 (7/396)	0.1 (1/912)	0.2 (2/817)
-11	0.8 (3/396)		
-14			0.1 (1/817)
-17	0.3 (1/396)	0.1 (1/912)	0.1 (1/817)
-35	0.3 (1/396)		
Additions			
Duplications			
+1	4.8 (19/396)		1.3 (11/817)
+4	2.3 (9/396)		
+19	0.3 (1/396)		
+28	0.3 (1/396)		
+48	0.3 (1/396)		
Insertions			
+1			0.2 (2/817)
Complex[b]			
-2			3.7 (30/817)
(Cryptic)[c]		0.1 (1/912)	7.5 (61/817)
-2, +bps			2.0 (16/817)
+1, +bps			1.2 (10/817)
Other			
Totals			
Deletions			
Hotspot	87.4 (346/396)	99.3 (906/912)	83.1 (679/817)
Other	4.0 (16/396)	0.5 (5/912)	1.0 (8/817)
Additions			
Duplications	7.8 (31/396)		1.3 (11/817)
Insertions			0.2 (2/817)
Complex			14.4 (117/817)
Other	0.8 (3/396)[d]		

[a] Deletion of either CG or GC from the sequence CGCGCGCG located at nucleotides 878–885.
[b] A frameshift mutation with an associated base substitution.
[c] A subset of complex frameshift mutations that appear as the deletion of either the CC or GG that flank the hotspot site (CCGCGCGCGG).
[d] No sequence available.

observed. Only 4% of mitomycin C- (KUPCHELLA and CEBULA 1990) and β-methoxy-acrolein- (O'HARA and MARNETT 1991) induced revertants had the hotspot mutation. Recently, we have shown that the chlorinated drinking water mutagen, MX, does not increase the frequency of the hotspot mutation above that observed in the background (DEMARINI *et al.* 1993). These three agents may interact with DNA in ways that are different from the mutagens described previously. Mitomycin C and β-methoxy-acrolein are cross-linking agents; the type of adduct that MX forms *in vivo* with DNA has not yet been characterized.

Mechanisms of hotspot mutations: The 2-base hotspot deletion among background revertants of the *hisD3052* allele might be explained most simply by the model of STREISINGER *et al.* (1966) and STREISINGER and OWEN (1985) in which misaligned replication intermediates, derived from slippage of one strand relative to the other, might be stabilized within iterated sequences. Indeed, the hotspot sequence provides more opportunity than does any other sequence within the target for the occurrence of slipped mispairing within an iterated sequence during replication.

The enhancement of this 2-base deletion by mutagens such as 4-AB that form DNA adducts at the C(8) position of guanine may then be explained by a correct incorporation/slippage model proposed by SCHAAPER *et al.* (1990) and tested experimentally by LAMBERT *et al.* (1991). This model is illustrated in Figure 4 in which cytosine is incorporated correctly opposite a 4-AB-adducted guanine; however, base pairing involving an adducted guanine may be unstable and/or progression of the DNA polymerase may be hindered by the adduct, increasing the probability of strand slippage on the repeated GpC motif. A new stabilized primer terminus is then formed, and extension of this terminus yields the 2-base hotspot deletion.

Evidence supporting this model includes theoretical and spectral studies showing that 4-AB adducts at the C(8) position of guanine can cause the adducted guanine to assume either the *anti* or *syn* conformation, and that while in the *anti* conformation, the adducted guanine can pair correctly with cytosine (BROYDE *et al.* 1985; SHAPIRO *et al.* 1986). The model's requirement for correct insertion opposite the adducted guanine to produce the hotspot mu-

TABLE 4

Estimated number of background and 4-AB-induced mutations in 4-AB spectra

Strain	Mutation class	Background frequency (%)[a]	Expected[b]	Observed[c]	Induced by 4-AB
TA1978	Hotspot	15	10	346	336
	Deletions	26	17	16	
	Duplications	59	38	31	
TA1538	Hotspot	50	25	906	881
	Deletions	34	17	5	
	Duplications	15	8	0	
	Complex	0	0	1	1
TA98	Hotspot	44	25	679	655
	Deletions	30	16	9	
	Duplications	18	10	10	
	Complex	8	5	119	114

[a] From DEMARINI *et al.* (1992) and in preparation. The average background rev/plate for the *hisD3052* strains were 44 (TA1978), 27 (TA1538), 13 (UTH8414), and 37 (TA98).

[b] The expected number of background mutations in each 4-AB spectrum was calculated by first dividing the total number of mutants analyzed by the fold over background (Figure 3) to obtain the estimated number of background mutations in the spectra. This number was then distributed among the mutant classes according to the frequency of the occurrence of the mutant classes in the background mutation spectra.

[c] From Table 3.

tation is consistent with studies of base insertion opposite other dG-C(8) adducts in which cytosine is the base inserted most frequently opposite the adducted guanine (RABKIN and STRAUSS 1984; MICHAELS *et al.* 1991).

Application of the model to the specific sequence of the hotspot leads to the prediction that adducts on G_2, G_3, G_4 or G_5 (but not on G_1) can produce the hotspot deletion (Figure 4). An adduct on G_1 may permit correct incorporation of a cytosine, but there is no suitable sequence 5′ of the adducted G_1 on which appropriate slippage can occur to produce a 2-base deletion. This model is similar to that suggested by LAMBERT *et al.* (1992a,b) for −1 frameshifts within a contiguous run of guanines.

The pathway delineated in Figure 4 is but one of a large number that can be drawn, all ultimately leading to the same observed 2-base deletion. These pathways differ by the number of nucleotides incorporated following the insertion of a C opposite the adducted G and by the precise conformation assumed following the 2-base slippage. For example, in the case of the depicted G_3 adduct, either 0, 1, 2, or 3 subsequent nucleotides could be incorporated prior to slippage. All cases would result in the same observed 2-base deletion. Furthermore, following slippage, the misaligned intermediate could assume one of several conformations in which the adducted G_3 is either intra- or extrahelical. In this regard, GARCIA *et al.* (1993) have shown that a monotonic run of guanines containing a 2-AAF adduct was stabilized when the adducted guanine was extrahelical.

At this time, we have no strong arguments to favor one specific pathway over the other. Instead, we wish to stress that all pathways proceed by a common mechanism comprised of (1) the incorporation of a C opposite the adducted G and (2) a subsequent 2-base slippage promoted and directed by the relative instability of the primer terminus and the specific sequence context. It is likely that the high degeneracy of the intermediate state is a contributing factor to the high frequency of the −2 event, in conjunction with a total of eight Gs (four in each strand) as targets for adduction that could be potential initiators of the event.

The repeated GpC motif within the hotspot may permit additional mechanisms to operate. Such sequences can form Z-DNA, which is unstable and may result in a high frequency of spontaneous 2-base deletions (FREUND *et al.* 1989). The formation of Z-DNA by the presence of this motif three times within the hotspot sequence may account for the high background frequency of 2-base deletions at the *hisD3052* allele. Theoretical and spectroscopic studies by BROYDE *et al.* (1985) and SHAPIRO *et al.* (1986) indicate that 4-AB guanine adducts at the C(8) position can readily adopt the *syn* conformation, which may promote the B- to Z-DNA transition in a manner similar to that proposed for 2-acetylaminofluorene (BURNOUF *et al.* 1989). Support for this suggestion comes from ABUAF *et al.* (1987) who showed by circular dichroism that modification of poly(dG-dC) by a reactive form of 4-AB induced the B- to Z-DNA transition. Thus, the 2-base hotspot deletion may result from the structural features of Z-DNA and/or the action of certain Z-DNA-binding proteins (*e.g.*, FISHEL *et al.* 1988) on such structures, especially on C(8) adducts on guanine in Z-DNA. The importance of the DNA sequence context is illustrated by the finding that 4-AB adducts in a 15-mer duplex not containing a repeating GpC motif yield a DNA polymer that has primarily a B-conformation (MARQUES and BELAND 1990; CHO *et al.* 1992).

Mechanism of complex frameshifts: The model described above (Figure 4) for the hotspot deletion (*i.e.*, correct incorporation of a cytosine opposite an adducted guanine followed by slippage) can be modified to involve misincorporation opposite an adducted guanine followed by slippage to explain the complex frameshifts (Figure 5). This model is based on (1) the for-

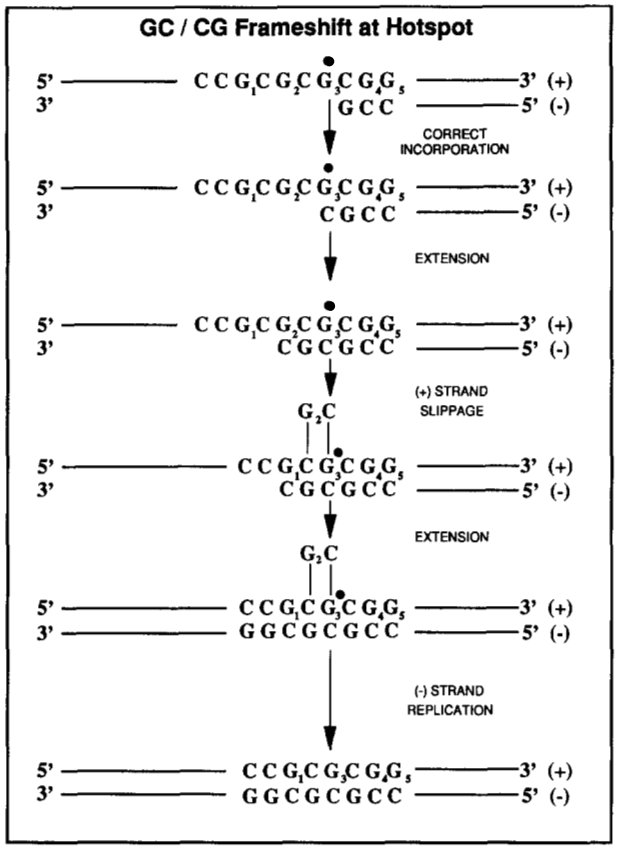

FIGURE 4.—Proposed mechanism of hotspot deletion involving correct incorporation of a cytosine opposite a 4-AB-adducted guanine. Such base pairs may be unstable and/or progression of the DNA polymerase may be hindered by the adduct, increasing the probability of strand slippage on the repeated GpC motif. A new stabilized primer terminus is then formed, and extension of this terminus yields the 2-base hotspot deletion.

mation of DNA adducts by 4-AB in Salmonella predominantly at the C(8) position of guanine (KADLUBAR *et al.* 1982), (2) the finding that such adducts cause the guanines in the majority of 4-AB-adducted poly (CpG) molecules (a sequence motif found at the complex frameshift hotspot) to reside in the *syn* conformation (BROYDE *et al.* 1985; SHAPIRO *et al.* 1986), (3) the possibility for the O^6 and N-7 atoms of modified guanines in the *syn* conformation to mispair with the N-1 and N^2 of guanine or with the N^6 and N-1 of adenine, resulting in transversions (DRAKE and BALTZ 1976; TOPAL and FRESCO 1976), (4) the observation that in the presence of pKM101, ~80% of the 4-AB-induced base substitutions are transversions (Figure 2), and (5) the well documented ability of DNA polymerases (when copying undamaged templates *in vitro*) to produce frameshift errors that are mediated by a nucleotide misinsertion and a subsequent slippage event (KUNKEL and SONI 1988; BEBENEK and KUNKEL 1990; KUNKEL 1990; BEBENEK *et al.* 1992).

Nearly all of the complex frameshifts in the 4-AB mutation spectrum in TA98 are accounted for by our proposed misincorporation/slippage model. The four general categories of complex frameshifts that are explained by the model are illustrated in Figure 5 and discussed below.

For complex frameshifts at the hotspot, which generally consist of 2-base deletions and a contiguous base substitution, we postulate that (1) misincorporation occurs opposite an adducted guanine, (2) two or more additional (correct) bases are incorporated, (3) a 2-base slippage occurs on the adducted strand, (4) extension continues, and (5) replication of the nonadducted strand results in a complex frameshift consisting of a 2-base deletion and a contiguous base substitution (Figure 5A). The model predicts that adducts on only G_3, G_4 or G_5 can participate in the generation of these complex frameshifts. As stated previously for the 2-base deletion at the hotspot site, the possible intermediates that can be drawn are numerous, depending on the extent of synthesis following misincorporation (1, 2, or 3 nucleotides in the case of an adducted G_3) and the precise nature of the bases in the bulge.

An additional feature of the 4-AB-induced mutation spectrum in strain TA98 is the presence of two clusters of mutations flanking the hotspot (Figure 3): the apparent deletion of CC at the 5′ end of the hotspot region, and the apparent deletion of GG at the 3′ end of the hotspot region (CCGCGCGCGG). Although these mutations appear at first to be simple 2-base deletions, they are not explicable by simple slippage models because there is no additional CC or GG sequence adjacent to the two sites on which an appropriate 2-base slippage can occur. The absence of these two mutations from the 4-AB-induced mutation spectra in the two pKM101-minus strains (TA1978 and TA1538), as well as their rare occurrence among background revertants of TA1978 and TA1538 (in preparation), suggest that the frequency of these mutations is enhanced by the presence of the pKM101 plasmid and that these mutations may be complex mutations in disguise (*i.e.*, cryptic complex frameshifts).

Indeed, the cryptic complex frameshifts may be explained in the same way as the other complex frameshifts; however, they represent a restricted set of complex frameshifts at the hotspot site. The model predicts that these mutations occur when a guanine is misincorporated opposite an adducted G_5, followed by a 2-base slippage. Misincorporation of a guanine opposite an adducted G_5 residing on the nontranscribed (−) strand, followed by a 2-base slippage, produces the –CC mutation (Figure 5B); misincorporation of a guanine opposite an adducted G_5 on the transcribed (+) strand, followed by a 2-base slippage, produces the –GG mutation (Figure 5C).

In contrast to the complex frameshifts at the hotspot, which generally consist of a 2-base deletion and a contiguous base substitution, the complex frameshifts at or

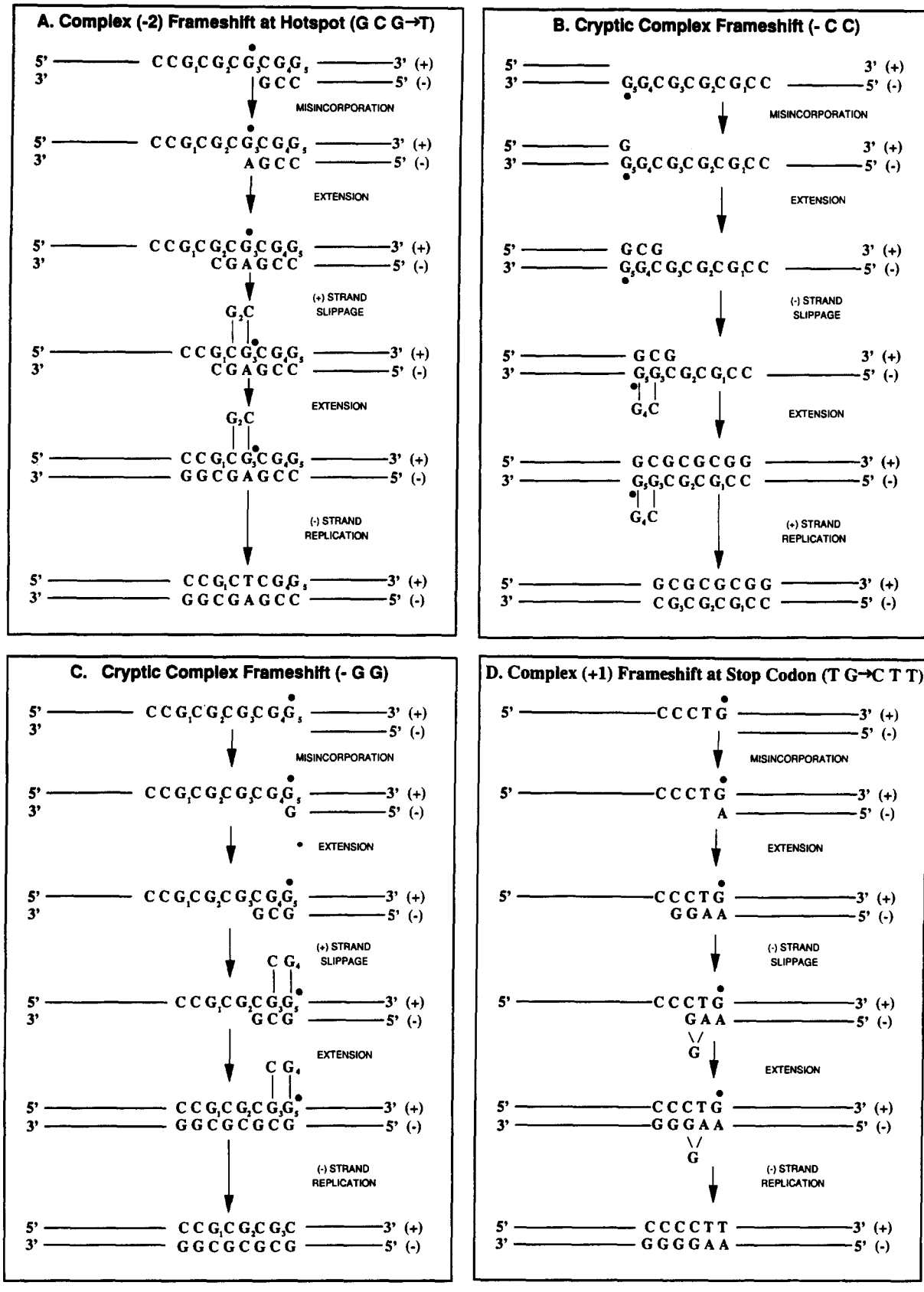

FIGURE 5.—Illustration of the misincorporation/slippage model for (A) a common complex frameshift at the hotspot, (B) the –CC cryptic complex frameshift at the hotspot, (C) the –GG cryptic complex frameshift at the hotspot, and (D) a common complex frameshift at the stop codon.

TABLE 5

Distribution and frequency of deletions and misincorporations among complex frameshifts at hotspot site (nucleotides 877–886)

	Location of adduct		Deletion 5′ of adduct			Misincorporated base opposite adduct	
Mutation	Strand	Guanine[a]	Strand	CG	GC	Base	No.
ΔCC 877–878	–	5	–	CG		G	23
Δ877–879 +A	–	5	–	CG		A	11
Δ878–880 +A	–	4	–		GC	A	26
Δ878–880 +T	–	4	–		GC	T	5
Δ878–880 +G	–	4	–		GC	G	2
Δ880–882 +A	–	3	–		GC	A	8
Δ880–882 +T	–	3	–		GC	T	1
Δ880–882 +G	–	3	–		GC	G	1
Δ881–883 +T	+	3	+		GC	A	1
Δ883–885 +A	+	4	+		GC	T	2
Δ883–885 +C	+	4	+		GC	G	1
Δ884–886 +T	+	5	+	CG		A	2
Δ884–886 +A	+	5	+	CG		T	1
ΔGG 885–886	+	5	+	CG		G	7

[a] Adducts numbered as in Figure 4.

near the TGA stop codon 3′ of the hotspot involve a 1-base duplication and a base substitution separated by one base. The misincorporation/slippage model explains these mutations by postulating that after misincorporation, a 1-base slippage occurs on the nonadducted strand (as opposed to a 2-base slippage on the adducted strand for the complex frameshifts at the hotspot). Extension followed by replication produces a 1-base duplication and a base substitution separated by one nucleotide. Figure 5D illustrates the model for the most common mutation of this category.

Application of the misincorporation/slippage model to all of the complex frameshifts at the hotspot site, including the cryptic complex frameshifts, permits an analysis of the relative frequency at which misincorporation/slippage events occur at each of the nucleotides in the two strands, as well as the preference of misincorporation at each of these sites. The results (Table 5 and Figure 6A) show that there is a clear strand bias, such that 84% of the complex frameshifts at the hotspot are due to misincorporations opposite adducted guanines located on the nontranscribed (–) strand. This may be due to (1) the presence of more 4-AB adducts on the nontranscribed (–) strand than on the transcribed (+) strand, (2) a replication asymmetry that causes adducts on the lagging strand to be more mutagenic than those on the leading strand (Veaute and Fuchs 1993), or (3) DNA sequence context effects that extend beyond the immediately adjacent nucleotides.

Application of the model also predicts that adducts located on guanines at the 3′ end of the sequence (*i.e.*, G_5) account for more of the mutations than do those located at the 5′ end of the sequence (G_3) (Table 5, Figure 6B). This observation is reminiscent of the greater mutagenic effectiveness of adducts at the 3′ end of a contiguous run of guanines in *E. coli* as demonstrated by Lambert *et al.* (1992b). Perhaps adducts located at the 3′ end of an iterated sequence provide a greater number of slipped intermediates than would adducts located at the 5′ end of the sequence. Slipped intermediates resulting from 3′ adducts may also be more stable due to the availability for base pairing of more sequence 5′ to the slipped site.

Application of the model to the complex frameshifts at the hotspot also shows that the polymerase preferentially misincorporates adenine at $G_3 + G_4$: A (74%) > T (17%) > G (9%) (Table 5, Figure 6C). These relative frequencies of misincorporation in the presence of pKM101 at the hotspot of the frameshift allele *hisD3052* in strain TA98 are similar to those produced by 4-AB in the presence of pKM101 at the base substitution allele *hisG46* allele in strain TA100 (Figure 2): A (79%) > T (20%) > G (1%). This is consistent with the role of the pKM101 plasmid in facilitating error-prone translesion synthesis, resulting in these base substitutions at both alleles.

Application of the model to the complex frameshifts resulting from 4-AB adducts on G_5 reveals the following relative frequencies of misincorporation: G (68%) > A (30%) > T (2%) (Table 5, Figure 6C). These values suggest a high frequency of misincorporation of guanine opposite an adducted G_5, which leads to the production of the cryptic complex frameshifts. The sequence context of G_5 is different from that of G_4 and G_3, which could affect misincorporation ratios as well as slippage tendencies. We note that in a different DNA sequence context (*hisG46*), there was no evidence for the misincorporation of guanine opposite a 4-AB-adducted guanine because 4-AB did not induce GC → CG transversions at the *hisG46* allele (Figure 2). Figure 7 illustrates the polarity of adduction/misincorporation and the frequency with which different nucleotides may be misincorporated opposite specific adducted guanines in a manner consistent with the model and the 4-AB-induced TA98 mutation spectrum.

Our recovery of one complex frameshift mutation in a plasmid-minus strain (TA1538), along with the recovery of several cryptic complex frameshifts among spontaneous revertants of TA1978 and TA1538 (D. M.

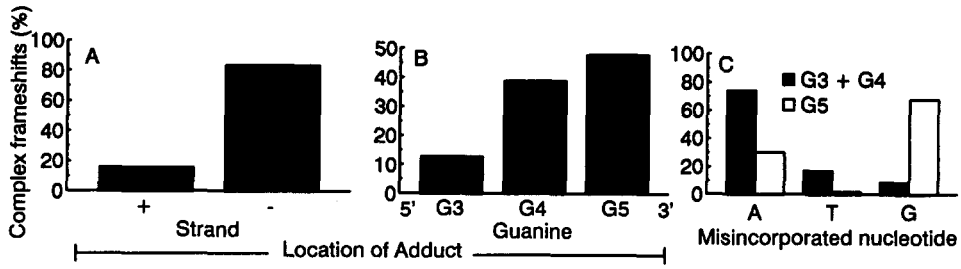

FIGURE 6.—Location of 4-AB-adducted guanines and the frequency of misincorporated nucleotides predicted by application of the misincorporation/slippage model to the complex frameshifts at the hotspot.

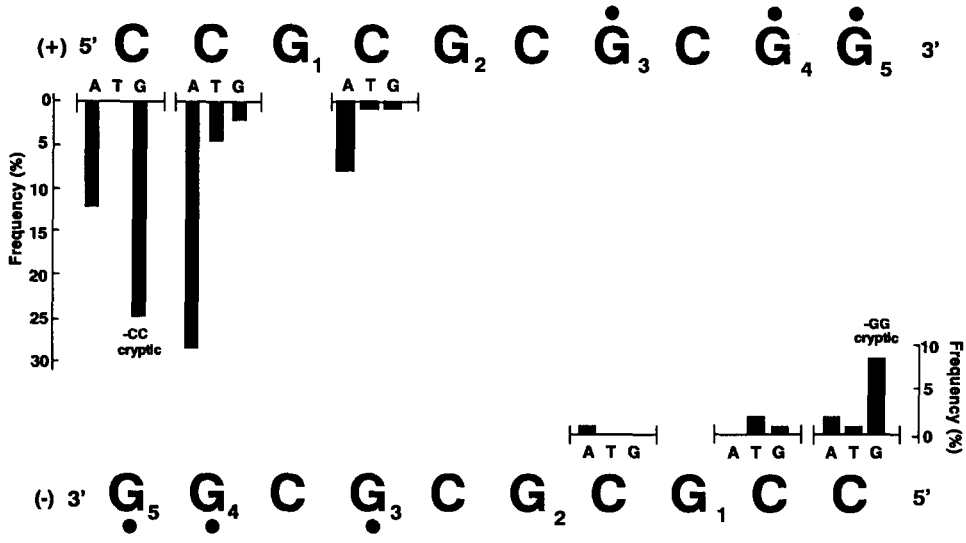

FIGURE 7.—Location and frequency of misincorporated nucleotides predicted by application of misincorporation/slippage model to the complex frameshifts at the hotspot.

DEMARINI, manuscript in preparation) indicates that the pKM101 plasmid is not absolutely required for the production of complex frameshifts. In the absence of the plasmid, these mutations may be mediated by SOS functions that are present at a low level in pKM101-minus strains of Salmonella (EISENSTADT 1987; SMITH and EISENSTADT 1989; SMITH *et al.* 1990; NOHMI *et al.* 1991; WOODGATE *et al.* 1991). However, the present study demonstrates clearly that the pKM101 plasmid greatly enhances the production of complex frameshift mutations. The pKM101 plasmid contains the *mucAB* genes, which appear to be at least partial functional analogues of the *E. coli umuDC* genes, which participate in the SOS response in *E. coli* (WALKER 1984; BLANCO *et al.* 1986).

Previous observations are consistent with the conclusion that pKM101 enhances the production of complex frameshift mutations. FELTON *et al.* (1989) recovered two benzo(*a*)pyrene-induced complex frameshift mutations in strain TA98 (out of an unspecified total) but none out of 24 benzo(*a*)pyrene-induced revertants of the plasmid-minus strain TA1538. CEBULA and KOCH (1991) reported the recovery of complex frameshift mutations that may have been promoted by pKM101 or other SOS functions in frameshift strains of Salmonella. O'HARA and MARNETT (1991) found no complex frameshifts among 37 background or 27 mutagen-induced revertants of the *hisD3052* allele in a pKM101-minus strain of Salmonella. In *E. coli* bacteriophage M13, the ability of SOS, induced by UV irradiation or the *mucAB*-containing plasmid pGW270, to enhance aflatoxin B1 (AFB1)-induced complex mutations has also been noted (REFOLO *et al.* 1987; SAMBAMURTI *et al.* 1988; SAHASRABUDHE *et al.* 1989; BENNETT *et al.* 1988, 1991). Some of the mechanisms proposed to explain the AFB1-induced complex frameshifts in M13 (REFOLO *et al.* 1987) share features with the mechanisms proposed here for 4-AB-induced complex frameshifts in Salmonella.

Mutagenic potency as a function of mutational mechanisms: 4-AB displays a 60-fold (or larger) range of mutagenic potencies in the present study, depending on the DNA repair background of the strain of Salmonella and the allele used to measure the specificity (Table 1). Because the strains are otherwise isogenic, the differences in mutagenic potency at any one allele are likely due to the number of unrepaired adducts and the probability of the steps that are necessary to convert an adduct to a selectable mutation in each repair background. As discussed below, the mutagenic mechanisms derived from the mutation spectra can provide a framework for understanding the relative mutagenic potency of 4-AB among the different strains.

Reversion of the *hisD3052* frameshift allele may be initiated by 4-AB-adducted guanines that promote slipped/mispairing. In an excision repair-proficient background, there are relatively few unrepaired 4-AB-adducted guanines to promote the required incorporation and slippage events, and the added ability to perform error-prone synthesis past such adducts by the

addition of the pKM101 plasmid does not enhance the mutagenic potency. This is consistent with the view that most of the 4-AB-induced mutations at the *hisD3052* allele, *i.e.*, the hotspot CG or GC deletion, occur by correct incorporation of a C opposite 4-AB-adducted guanines. The addition of the Δ*uvrB* allele increases the number of 4-AB-adducted guanines available to promote slippage, leading to a strong enhancement of mutagenic potency. The potency is increased further by the addition of the pKM101 plasmid, which facilitates error-prone translesion synthesis. Although misincorporation by itself is insufficient to revert the frameshift allele, it produces a potentially unstable pairing that likely promotes slippage, causing an enhanced frameshift mutagenic potency.

For 4-AB to revert the *hisG46* base-substitution allele, error-prone synthesis past a misincorporated nucleotide opposite a 4-AB-adducted guanine is necessary to produce a revertant containing a base substitution and requires the pKM101 plasmid. The presence of more unrepaired 4-AB adducts due to *uvrB* enhances the probability of this event, leading to a 30-fold increase in mutagenic potency. This is roughly the enhancement in the mutagenic potency of 4-AB (40-fold) produced by *uvrB* at the frameshift allele. This suggests, perhaps, that there are 30–40 times more unrepaired 4-AB adducts present in *uvrB* strains compared to DNA excision repair-proficient strains. This conclusion for Salmonella is consistent with findings in *E. coli* for the repair of 4-AB adducts by the nucleotide excision-repair system (TAMURA and KING 1990; SUZUKI *et al.* 1993). The mutagenic efficiency of *N*-hydroxy-4-AB in a *uvrB* strain (TA1538) is ~6% (KADLUBAR *et al.* 1982; BELAND *et al.* 1983). The mutation spectra presented here would indicate that this value reflects the ability of 4-AB-adducted guanines (G_2, G_3, G_4 and G_5) within the hotspot to promote a 2-base slippage, leading to the hotspot deletion.

CONCLUSIONS

In the absence of pKM101, 4-AB induces almost exclusively (100% for TA1978 and 99.9% for TA1538) the 2-base hotspot deletion at the *hisD3052* allele. We propose that the formation by 4-AB of adducts at the C(8) position of guanines G_2, G_3, G_4 and G_5 within the repetitive CG/GC motif in the hotspot region promotes the hotspot mutation via the correct incorporation of a cytosine opposite the adducted guanine. This may result in a slightly unstable pairing and/or may hinder the progression of the DNA polymerase such that a 2-base slippage occurs (facilitated by the CG/GC repeat), leading to the 2-base hotspot deletion.

In the presence of pKM101, ~85% of the 4-AB-induced revertants of the *hisD3052* allele also contain the hotspot mutation; the remaining revertants contain complex frameshift mutations, which consist of a frameshift and a base substitution. The pKM101 plasmid greatly enhances the production of these events, from 0% in TA1978 and 0.1% in TA1538 to 15% in TA98. The sequence changes and their location suggest a mutational model that involves misincorporation/slippage. At the hotspot, the complex frameshifts consist primarily of a 2-base deletion and a base substitution. 4-AB-adducted guanines in the CG/GC motif within the hotspot region may reside in the *syn* or the *anti* conformation and, thus, may mispair. Application of the misincorporation/slippage model to the 4-AB-induced mutation spectrum in strain TA98 predicts the following relative frequencies of misincorporation opposite G_3 + G_4: A (74%) > T (17%) > G (9%). These values are similar to those produced by 4-AB in the presence of pKM101 at the base-substitution allele *hisG46*, and they are consistent with the A rule. The model also predicts a polarity of mutagenic effectiveness, with adducts at the 3′ end (*e.g.*, G_5) accounting for more of the complex frameshifts at the hotspot than adducts at G_3 or G_4. There is also a prediction of a strand bias, such that 84% of the complex frameshifts at the hotspot are due to adducts on the nontranscribed (–) strand.

The 4-AB mutation spectrum in the presence of the plasmid contains a class of mutations that we call cryptic complex frameshifts that appear as deletions of the CC and GG dinucleotides that flank the hotspot sequence. Because these mutations are induced by 4-AB only in the plasmid-containing strain, we explain their formation by the misincorporation of a guanine opposite an adducted G_5, followed by a 2-base slippage on the adduct-containing strand. Thus, these apparent 2-base deletions are actually due to a G·C → C·G transversion and a CG (or GC) deletion.

The same model accounts for most of the complex frameshifts outside of the hotspot region, which are explained by misincorporation of adenine or thymine opposite an adducted guanine followed by a 1-base slippage on the nonadducted strand. This results in a 1-base duplication and a base substitution.

Finally, the mutational mechanisms postulated here provide a framework for understanding the relative mutagenic potency of 4-AB in the different DNA repair backgrounds. The results suggest that, regardless of the allele, there might be 30–40 times more unrepaired 4-AB adducts in *uvrB* strains than in excision repair-proficient strains. The presence of the plasmid presumably facilitates translesion synthesis across mispaired adducted guanines. The instability of such mispairs may promote more slippage than occurs in the absence of such mispairs, resulting in the formation of complex frameshifts and an enhancement in mutagenic potency. The high GC content of the *hisD3052* target region (72%) and the presence of iterated sequences within this target, all acting in concert with DNA repair and replication enzymes, provide a rich substrate for 4-AB-adducted guanines to initiate the diversity of mutations observed in the present study.

We thank THOMAS A. CEBULA and colleagues, U.S. Food and Drug Administration, Washington, D.C., for generously sharing with us their protocol for identifying the CG/GC hotspot deletion by colony probe hybridization prior to publication. We express our appreciation to W. THOMAS ADAMS and THOMAS R. SKOPEK for providing us with their statistical program. We thank MELISSA L. SHELTON for helping to probe-hybridize the TA100 revertants; we thank DOUG WHITEHOUSE for assembling the *hisD3052* mutation spectra on the computer; and we thank LOUISE M. BALL for her advice. We thank CRAIG B. BENNETT, JAMES C. FUSCOE, THOMAS A. KUNKEL, IAIN B. LAMBERT, LYNN S. RIPLEY and JEFFREY A. ROSS for their helpful comments on the manuscript. This manuscript was prepared in part from a dissertation submitted by J.G.L. in partial fulfillment of the requirements for the Ph.D. degree at the University of North Carolina at Chapel Hill. This manuscript has been reviewed by the Health Effects Research Laboratory, U.S. Environmental Protection Agency, and approved for publication. Approval does not signify that the contents necessarily reflect the views and policies of the Agency, nor does mention of trade names or commercial products constitute endorsement or recommendation for use.

LITERATURE CITED

ABUAF, P. A., F. F. KADLUBAR and D. GRUNBERGER, 1987 Circular dichroism of poly(dG-dC) modified by the carcinogens *N*-methyl-4-aminoazobenzene or 4-aminobiphenyl. Nucleic Acids Res. **15:** 7125–7136.

ADAMS, W. T., and T. R. SKOPEK, 1987 Statistical test for the comparison of samples from mutational spectra. J. Mol. Biol. **194:** 391–390.

ASHBY J., and R. MOHAMMAD, 1988 UDS activity in the rat liver of the human carcinogens benzidine and 4-aminobiphenyl, and the rodent carcinogens 23,3′-dichlorobenzidine and direct black 38. Mutagenesis **3:** 69–71.

BEBENEK, K., and T. A. KUNKEL, 1990 Frameshift errors initiated by nucleotide misincorporation. Proc. Natl. Acad. Sci. USA **87:** 4946–4950.

BEBENEK, K., J. D. ROBERTS and T. A. KUNKEL, 1992 The effects of dNTP pool imbalances on frameshift fidelity during DNA replication. J. Biol. Chem. **267:** 3589–3596.

BELAND F. A., and F. F. KADLUBAR, 1990 Metabolic activation and DNA adducts of aromatic amines and nitroaromatic hydrocarbons, pp. 267–326 in *Handbook of Experimental Pharmacology Vol. 94/1 Chemical Carcinogenesis and Mutagenesis 1*, edited by C. S. COOPER, and P. L. GROVER. Springer-Verlag, Heidelberg.

BELAND, F. A., D. T. BERANEK, K. L. DOOLEY, R. H. HEFLICH and F. F. KADLUBAR, 1983 Arylamine-DNA adducts *in vitro* and *in vivo*: their role in bacterial mutagenesis and urinary bladder carcinogenesis. Environ. Health Perspect. **49:** 125–134.

BELL, D. A., J. G. LEVINE and D. M. DEMARINI, 1991 DNA sequence analysis of revertants of the *hisD3052* allele of *Salmonella typhimurium* TA98 using the polymerase chain reaction and direct sequencing: application to 1-nitropyrene-induced revertants. Mutat. Res. **252:** 35–44.

BENNETT, C. B., X. LUO, L. M. REFOLO and M. Z. HUMAYUN, 1988 Effects of SOS and MucAB functions on reactivation and mutagenesis of M13 replicative form DNA bearing bulky lesions. Mutat. Res. **202:** 223–234.

BENNETT, C. B., X. LUO and M. Z. HUMAYUN, 1991 Genetic requirements for frameshift reversion induced by bulky DNA adducts in M13 DNA. Mutat. Res. **249:** 19–27.

BLANCO, M., G. HERERRA and V. ALEXANDRE, 1986 Different efficiency of UmuDC and MucAB proteins in UV light induced mutagenesis in *Escherichia coli*. Mol. Gen. Genet. **205:** 234–239.

BOOKLAND, E. A., C. A. REZNIKOFF, M. LINDSTROM and S. SWAMINATHAN, 1992a Induction of thioguanine-resistant mutations in human uroepithelial cells by 4-aminobiphenyl and its *N*-hydroxy derivatives. Cancer Res. **52:** 1615–1621.

BOOKLAND, E. A., S. SWAMINATHAN, K. W. GILCHRIST, R. OYASU and C. A. RESNIKOFF, 1992b Tumorigenic transformation and neoplastic progression of human uroepithelial cells after exposure *in vitro* to 4-aminobiphenyl or its metabolites. Cancer Res. **52:** 1606–1614.

BROYDE, S., B. E. HINGERTY and A. R. SRINIVASAN, 1985 Influence of the carcinogen 4-aminobiphenyl on DNA conformation. Carcinogenesis **6:** 719–725.

BURNOUF, D., P. KOEHL and R. P. P. FUCHS, 1989 Single adduct mutagenesis: Strong effect of the position of a single acetylaminofluorene adduct within a mutation hot spot. Proc. Natl. Acad. Sci. USA **86:** 4147–4151.

CEBULA, T. A., and W. H. KOCH, 1990a Analysis of spontaneous and psoralen-induced *Salmonella typhimurium hisG46* revertants by oligodeoxyribonucleotide colony hybridization: use of psoralens to cross-link probes to target sequences. Mutat. Res. **229:** 79–87.

CEBULA, T. A., and W. H. KOCH, 1990b Sequence analysis of *Salmonella typhimurium* revertants, pp. 367–377 in *Mutations and the Environment, Part D: Carcinogenesis*, edited by M. L. MENDELSOHN, and R. J. ALBERTINI. Wiley-Liss, New York.

CEBULA, T. A., and W. H. KOCH, 1991 Polymerase chain reaction (PCR) and its application to mutational analysis, pp. 255–266 in *New Horizons in Biological Dosimetry*, edited by B. L. GLEDHILL and F. MAURO. Wiley-Liss, New York.

CHO, B. P., F. A. BELAND and M. M. MARQUES, 1992 NMR structural studies of a 15-mer DNA sequence from a *ras* protooncogene, modified at the first base of codon 61 with the carcinogen 4-aminobiphenyl. Biochemistry **31:** 9587–9602.

CLIET, I., E. FOURNIER, C. MELCION and A. CORDIER, 1989 *In vivo* micronucleus test using mouse hepatocytes. Mutat. Res. **216:** 321–326.

DEMARINI, D. M., A. ABU-SHAKRA, R. GUPTA, L. J. HENDEE and J. G. LEVINE, 1992 Molecular analysis of mutations induced by the intercalating agent ellipticine at the *hisD3052* allele of *Salmonella typhimurium* TA98. Environ. Mol. Mutagen. **20:** 12–18.

DEMARINI, D. M., D. A. BELL, J. G. LEVINE, M. L. SHELTON and A. ABU-SHAKRA, 1993 Molecular analysis of mutations induced at the *hisD3052* allele of Salmonella by single chemicals and complex mixtures. Environ. Health Perspect. **101** (Suppl. 3): 207–212.

DRAKE, J., and R. BALTZ, 1976 The biochemistry of mutagenesis. Annu. Rev. Biochem. **45:** 11–39.

EISENSTADT, E., 1987 Analysis of mutagenesis, pp. 1016–1033 in *Escherichia coli and Salmonella typhimurium Cellular and Molecular Biology*, edited by F. C. NEIDHARDT, J. L. INGRAHAM, K. B. LOW, B. MAGASANIK, M. SCHAECHTER and H. E. UMBARGER. American Society for Microbiology, Washington, D.C.

EISENSTADT, E., J. K. MILLER, L.-S. KAHNG and W. M. BARNES, 1989 Influence of *uvrB* and pKM101 on the spectrum of spontaneous, UV- and γ-ray-induced base substitutions that revert *hisG46* in *Salmonella typhimurium*. Mutat. Res. **210:** 113–125.

FELTON, J. S., R. WU, N. H. SHEN, S. K. HEALY and J. C. FUSCOE, 1989 A recombinant DNA method for understanding the mechanism of *Salmonella* reverse mutations: role of repair, pp. 319–325 in *Multilevel Health Effects Research from Molecules to Man*, edited by J. F. PARK, and R. A. PELROY. Battelle Press, Columbus, Ohio.

FISHEL, R. A., K. DETMER and A. RICH, 1988 Identification of homologous pairing and strand-exchange activity from a human tumor cell line based on Z-DNA affinity chromatography. Proc. Natl. Acad. Sci USA **85:** 36–40.

FOWLER, R. G., L. MCGINTY and K. E. MORTELMANS, 1979 Spontaneous mutational specificity of drug resistance plasmid pKM101 in *Escherichia coli*. J. Bacteriol. **140:** 929–937.

FREUND, A.-M., M. BICHARA and R. P. P. FUCHS, 1989 Z-forming sequences are spontaneous deletion hotspots. Proc. Natl. Acad. Sci. USA **86:** 7465–7469.

FUSCOE, J. C., R. WU, N. H. SHEN, S. K. HEALY and J. S. FELTON, 1988 Base-change analysis of revertants of the *hisD3052* allele in *Salmonella typhimurium*. Mutat. Res. **201:** 241–251.

GARCIA, A., I. B. LAMBERT and R. P. P. FUCHS, 1993 DNA adduct-induced stabilization of slipped frameshift intermediates within repetitive sequences: implications for mutagenesis. Proc. Natl. Acad. Sci. USA **90:** 5989–5993.

HARTMAN, P. E., B. N. AMES, J. R. ROTH, W. M. BARNES and D. E. LEVIN, 1986 Target sequences for mutagenesis in Salmonella histidine-requiring mutants. Environ. Mutagen. **8:** 631–641.

HAWORTH, S., T. LAWLOR, K. MORTELMANS, W. SPECK and E. ZEIGER,

1983 Salmonella mutagenicity test results for 250 chemicals. Environ. Mutagen. **5** (Suppl. 1): 3–142.

IARC, 1987A *IARC Monographs on the Evaluation of Carcinogenic Risks to Humans, Suppl. 6, Genetic and Related Effects: An Updating of Selected IARC Monographs from Volumes 1–42.* International Agency for Research on Cancer, Lyon, France.

IARC, 1987B *IARC Monographs on the Evaluation of Carcinogenic Risks to Humans, Suppl. 7, Overall Evaluations of Carcinogenicity: An Updating of IARC Monographs Volumes 1–42.* International Agency for Research on Cancer, Lyon, France.

INMAN, M. A., M. A. BUTLER, T. H. CONNOR and T. S. MATNEY, 1983 The effects of excision repair and the plasmid pKM101 on the induction of His^+ revertants by chemical agents in *Salmonella typhimurium.* Teratogen. Carcinogen. Mutagen. **3:** 491–501.

IOANNIDES, C., D. F. V. LEWIS, J. TRINICK, S. NEVILLE, N. N. SERTKAYA, M. KAJBAF and J. W. GORROD, 1989 A rationale for the non-mutagenicity of 2- and 3-aminobiphenyls. Carcinogenesis **10:** 1403–1407.

ISONO, K., and J. YOURNO, 1974 Chemical carcinogens as frameshift mutagens: Salmonella DNA sequence sensitive to mutagenesis by polycyclic carcinogens. Proc. Natl. Acad. Sci. USA **71:** 1612–1617.

KADLUBAR, F. F., F. A. BELAND, D. T. BERANEK, K. L. DOOLEY, R. H. HEFLICH and F. E. EVANS, 1982 Arylamine-DNA adduct formation in relation to urinary bladder carcinogenesis and *Salmonella typhimurium* mutagenesis, pp. 385–396 in *Environmental Mutagens and Carcinogens*, edited by T. SUGIMURA, S. KONDO and H. TAKEBE. Alan R. Liss, New York.

KADLUBAR, F. F., K. L. DOOLEY, C. H. TEITEL, D. W. ROBERTS, R. W. BENSON, M. A. BUTLER, J. R. BAILEY, J. F. YOUNG, P. W. SKIPPER and S. R. TANNENBAUM, 1991 Frequency of urination and its effects on metabolism, pharmacokinetics, blood hemoglobin adduct formation, and liver and urinary bladder DNA levels in beagle dogs given the carcinogen 4-aminobiphenyl. Cancer Res. **51:** 4371–4377.

KIER, L. E., D. J. BRUSICK, A. E. AULETTA, E. S. VON HALLE, M. M. BROWN, V. F. SIMMON, V. DUNKEL, J. MCCANN, K. MORTELMANS, M. PRIVAL, T. K. RAO and V. RAY, 1986 *Salmonella typhimurium*/mammalian microsomal assay, A report of the U. S. Environmental Protection Agency Gene-Tox Program. Mutat. Res. **186:** 69–240.

KUNKEL, T. A., 1990 Misalignment-mediated DNA synthesis errors. Biochemistry **29:** 8003–8011.

KUNKEL, T. A., and A. SONI, 1988 Mutagenesis by transient misalignment. J. Biol. Chem. **263:** 14784–14789.

KUPCHELLA, E., and T. A. CEBULA, 1991 Analysis of *Salmonella typhimurium hisD3052* revertants: The use of oligodeoxyribonucleotide colony hybridization, PCR, and direct sequencing in mutational analysis. Environ. Mol. Mutagen. **18:** 224–230.

KUPCHELLA, E., W. H. KOCH and T. A. CEBULA, 1994 Mutant alleles of $tRNA^{Thr}$ genes suppress the *hisG46* missense mutation in *Salmonella typhimurium.* Environ. Mol. Mutagen. (in press).

LAMBERT, I. B., A. J. E. GORDON, D. W. BRYANT, B. W. GLICKMAN and D. R. MCCALLA, 1991 The action of 1-nitroso-8-nitropyrene in *Escherichia coli*: DNA adduct formation and mutational consequences in the absence of nucleotide excision-repair. Carcinogenesis **12:** 909–927.

LAMBERT, I. B., A. J. E. GORDON, B. W. GLICKMAN and D. R. MCCALLA, 1992a The influence of local DNA sequence and DNA repair background on the mutational specificity of 1-nitroso-8-nitropyrene in *Escherichia coli*: inferences for mutagenic mechanisms. Genetics **132:** 911–927.

LAMBERT, I. B., R. L. NAPOLITANO and R. P. P. FUCHS, 1992b Carcinogen-induced frameshift mutagenesis in repetitive sequences. Proc. Natl. Acad. Sci. USA **89:** 1310–1314.

LASKO, D. D., S. C. HARVEY, S. B. MALAIKAL, F. F. KADLUBAR and J. M. ESSIGMANN, 1988 Specificity of mutagenesis by 4-aminobiphenyl. J. Biol. Chem. **263:** 15429–15435.

MARON, D. M., and B. N. AMES, 1983 Revised methods for the Salmonella mutagenicity test. Mutat. Res. **113:** 173–215.

MARQUES, M. M., and F. A. BELAND, 1990 Synthesis, characterization, and solution properties of *ras* sequences modified by arylamine carcinogens at the first base of codon 61. Chem. Res. Toxicol. **3:** 559–565.

MATTERN, I. E., F. P. OLTHOFF-SMIT, B. L. M. JACOBS-MEIJSING, B. E. ENGER-VALK, P. H. POUWELS and P. H. M. LOHMAN, 1985 A system to determine basepair substitutions at the molecular level, based on restriction enzyme analysis; influence of the *muc* genes of pKM101 on the specificity of mutation induction in *E. coli.* Mutat. Res. **148:** 35–45.

MICHAELS, M. L., T. M. REID, C. M. KING and L. J. ROMANO, 1991 Accurate *in vitro* translesion synthesis by *Escherichia coli* DNA polymerase I (large fragment) on a site-specific, aminofluorene-modified oligonucleotide. Carcinogenesis **12:** 1641–1646.

NOHMI, T., A. NAKURA, Y. NAKAI, M. WATANABE, S. Y. MURAYAMA and T. SOFUNI, 1991 *Salmonella typhimurium* has two homologous but different *umuDC* operons: cloning of a new *umuDC*-like operon (*samAB*) present in a 60-megadalton cryptic plasmid of *S. typhimurium.* J. Bacteriol. **173:** 1051–1063.

OESCHGER, N. S., and P. E. HARTMAN, 1970 ICR-induced frameshift mutations in the histidine operon of Salmonella. J. Bacteriol. **101:** 490–504.

O'HARA, S. M., and L. J. MARNETT, 1991 DNA sequence analysis of spontaneous and β-methoxy-acrolein-induced mutations in *Salmonella typhimurium hisD3052.* Mutat. Res. **247:** 45–56.

OLLER, A. R., P. RASTOGI, S. MORGANTHALER and W. G. THILLY, 1989 A statistical model to estimate variance in long term-low dose mutation assays; testing of the model in a human lymphoblastoid mutation assay. Mutat. Res. **216:** 149–161.

PRIVAL, M. J., and T. A. CEBULA, 1992 Sequence analysis of mutations arising during prolonged starvation of *Salmonella typhimurium.* Genetics **132:** 303–310.

RABKIN, S. D., and B. S. STRAUSS, 1984 A role for DNA polymerase in the specificity of nucleotide incorporation opposite *N*-acetyl-2-aminofluorene adducts. J. Mol. Biol. **178:** 569–594.

REFOLO, L. M., C. B. BENNETT and M. Z. HUMAYUN, 1987 Mechanisms of frameshift mutagenesis by aflatoxin β_1-2,3-dichloride. J. Mol. Biol. **193:** 609–636.

RIPLEY, L. S., 1990 Frameshift mutation: determinants of specificity. Annu. Rev. Genet. **24:** 189–213.

SAHASRABUDHE, S., K. SAMBAMURTI and M. Z. HUMAYUN, 1989 Mutagenesis by aflatoxin in M13 DNA: base-substitution mechanisms and the origin of strand bias. Mol. Gen. Genet. **217:** 20–25.

SAMBAMURTI, K., J. CALLAHAN, X. LUO, C. P. PERKINS, J. S. JACOBSON and M. Z. HUMAYUN, 1988 Mechanisms of mutagenesis by a bulky DNA lesion at the guanine N7 position. Genetics **120:** 863–873.

SANGER, F., S. NICKLEN and A. R. COULSON, 1977 DNA sequencing with chain-terminating inhibitors. Proc. Natl. Acad. Sci. USA **74:** 5463–5467.

SCHAAPER, R. M., N. KOFFEL-SCHWARTZ and R. P. P. FUCHS, 1990 *N*-Acetoxy-*N*-acetyl-2-aminofluorene-induced mutagenesis in the *lacI* gene of *Escherichia coli.* Carcinogenesis **11:** 1087–1095.

SHAPIRO, R., G. R. UNDERWOOD, H. ZAWADZKA, S. BROYDE and B. E. HINGERTY, 1986 Conformation of d(CpG) modified by the carcinogen 4-aminobiphenyl: a combined experimental and theoretical analysis. Biochemistry **25:** 2198–2205.

SHELBY, M. D., D. K. GULATI, R. R. TICE and J. P. WOJCIECHOWSKI, 1989 Results of tests for micronuclei and chromosomal aberrations in mouse bone marrow cells with the human carcinogens 4-aminobiphenyl, treosulphan, and melphalan. Environ. Mol. Mutagen. **13:** 339–342.

SMITH, C. M., and E. EISENSTADT, 1989 Identification of a *umuDC* locus in *Salmonella typhimurium* LT2. J. Bacteriol. **171:** 3860–3865.

SMITH, C. M., W. H. KOCH, S. B. FRANKLIN, P. L. FOSTER, T. A. CEBULA and E. EISENSTADT, 1990 Sequence analysis and mapping of the *Salmonella typhimurium* LT2 *umuDC* operon. J. Bacteriol. **172:** 4964–4978.

STEELE, C. M., and C. IOANNIDES, 1986 Induction of rat hepatic mixed function oxidases by aromatic amines and its relationship to their bioactivation to mutagens. Mutat. Res. **162:** 41–46.

STEINMETZ, K. L., C. E. GREEN, J. P. BAKKE, D. K. SPAK and J. C. MIRSALIS, 1988 Induction of unscheduled DNA synthesis in primary cultures of rat, mouse, hamster and human hepatocytes. Mutat. Res. **206:** 91–102.

STREISINGER, G., and J. OWEN, 1985 Mechanisms of spontaneous and induced frameshift mutation in bacteriophage T4. Genetics **109:** 633–659.

STREISINGER, G., Y. OKADA, J. EMRICH, J. NEWTON, A. TSUGITA, E. TERZAGHI

and M. INOUYE, 1966 Frameshift mutations and the genetic code. Cold Spring Harbor Symp. Quant. Biol. **31:** 77–84.

SUZUKI, M., K. TAKAHASHI, T. MORITA, M. KOJIMA and M. TADA, 1993 The action of 4-hydroxyaminobiphenyl in *Escherichia coli*: cytotoxic and mutagenic effects in DNA repair deficient strains. Mutat. Res. **301:** 125–134.

TAMURA, N., and C. M. KING, 1990 Comparative survival of aminobiphenyl- and aminofluorene-substituted plasmid DNA in *Escherichia coli* Uvr endonuclease deficient strains. Carcinogenesis **11:** 535–540.

TOPAL, M. D., and J. R. FRESCO, 1976 Complementary base pairing and the origin of substitution mutations. Nature **263:** 285–289.

TRIPATHY, N. K., F. E. WURGLER and H. FREI, 1990 Genetic toxicity of six carcinogens and six non-carcinogens in the Drosophila wing spot test. Mutat. Res. **242:** 169–180.

VEAUTE, X., and R. P. P. FUCHS, 1993 Greater susceptibility to mutations in lagging strand of DNA replication in *Escherichia coli* than in leading strand. Science **261:** 598–600.

WALKER, G. W., 1984 Mutagenesis and inducible responses to deoxyribonucleic acid damage in *Escherichia coli*. Microbiol. Rev. **48:** 60–93.

WOODGATE, R., A. S. LEVINE, W. H. KOCH, T. A. CEBULA and E. EISENSTADT, 1991 Induction and cleavage of *Salmonella typhimurium* UmuD protein. Mol. Gen. Genet. **229:** 81–85.

Communicating editor: N. R. DRINKWATER